



## CHARACTERISTICS OF PINE NEEDLES EXPOSED TO POLLUTION IN SILESIA, POLAND: CARBON ISOTOPES, IWUE, AND TRACE ELEMENT CONCENTRATIONS IN PINE NEEDLES

Barbara Sensuła<sup>1\*</sup>  • Natalia Piotrowska<sup>1</sup>  • Katarzyna Nowińska<sup>2</sup> • Michał Koruszowicz<sup>1</sup> • Dawid Łazaj<sup>1</sup> • Rafał Osadnik<sup>1</sup> • Radosław Paluch<sup>1</sup> • Adam Stasiak<sup>1</sup> • Beniamin Strączek<sup>1</sup>

<sup>1</sup>The Silesian University of Technology, Institute of Physics – Center for Science and Education, Konarskiego 22B, Gliwice 44-100, Poland

<sup>2</sup>The Silesian University of Technology, Faculty of Mining, Safety Engineering and Industrial Automation, Department of Applied Geology, Akademicka 2, Gliwice 44-100, Poland

**ABSTRACT.** Here, we present the results of carbon isotope and elemental analysis of one-year-old *Pinus Sylvestris* L. needles collected in 2021 from 10 sampling sites in a highly populated and industrialized area of Poland. The needles were exposed to air pollution for one year. The chemical analysis of the samples was performed using different methods: radiocarbon analysis by accelerator mass spectrometry, stable isotope analysis using isotope ratio mass spectrometry, and elemental analysis by inductively coupled plasma-atomic emission spectroscopy. Variations in the carbon isotopes and elemental composition of pine needles were due to a mixture of carbon dioxide originating from different sources such as households, vehicle traffic, and industrial factories.

**KEYWORDS:** carbon isotopes, iWUE, pine needles, pollution, trace elements.

### INTRODUCTION

CO<sub>2</sub> emitted during the combustion of fossil fuels (Suess 1955) contains no <sup>14</sup>CO<sub>2</sub> and is depleted in <sup>13</sup>CO<sub>2</sub>. Trees assimilate CO<sub>2</sub> via stomata in their leaves. Carbon isotopes are not retranslocated after fixation into the structure of the needle (when the growth process is over) (Barszczowska and Jędrysek 2005). Due to a mixture of CO<sub>2</sub> originating from different sources, variations in <sup>14</sup>C and <sup>13</sup>C in atmospheric carbon dioxide can be reflected in the isotopic composition of trees (Suess 1955; Keeling 1973; Rakowski 2011; Pazdur et al. 2013). Moreover, gaseous and dust air contaminants associated with different human activities, such as industry, road transport, low and high-stack emission, may impact the photosynthesis rate (*A*) and stomatal conductance (*g<sub>s</sub>*), which indicate leaf transpiration and affect the water use efficiency (WUE), which is defined as the relation between water used to fix the carbon. Intrinsic WUE (iWUE) relates photosynthesis to the stomatal conductance of water. Physiological responses of trees to the air pollution is usually connected with changing the stomata conductivity and photosynthesis rate, which results in higher δ<sup>13</sup>C values in tree rings and leaf tissues. The photosynthesis rate and the conductivity of the stomata can be influenced by many factors: climatic (temperature, drought increase) and anthropogenic (e.g., an increase in SO<sub>2</sub> and O<sub>3</sub> reduces conductivity and at the same time inhibits the photosynthesis process, while the photosynthesis rate may be increased during short-term exposure to increased NO<sub>x</sub> concentration (Cherubini et al. 2021). The impact of pollutants in the most industrialized part of Poland, Silesia, on the tree conditions, including changes in the width of annual tree growth and changes in the isotopic and elemental composition of annual shoots and pine (*Pinus Sylvestris* L.) wood, has been the subject of previous studies (for example: Sensuła et al. 2015, 2018, 2021; Piotrowska et al. 2020). Analyses made in the last decade have shown a high concentration of <sup>14</sup>C in Silesia (higher concentration than those of “clean” air, as well as variations in the carbon isotopic composition of plants, water use efficiency, and elemental composition.

\*Corresponding author. Email: [Barbara.sensula@polsl.pl](mailto:Barbara.sensula@polsl.pl)

During our investigations in 2012–2014 in Silesia (Sensula et al. 2015, 2018, 2021), we noted a higher radiocarbon concentration in foliage and tree rings in pine trees grown in the forests in the industrial area of Silesia compared with the concentration in clean air based on data from Jungfraujoch (Hammer et al. 2017); this phenomenon has not been explained yet and requires more detailed analysis of the carbon cycle in this area. We cannot exclude underestimation of the Suess effect for all investigated sites. Many factors affect biological and physical processes controlling the carbon cycle, for example heterotrophic respiration, biomass burning, oceanic CO<sub>2</sub> sources, and nuclear-industry-produced <sup>14</sup>C. In the Silesia we can exclude the two latter ones, however, CO<sub>2</sub> emissions from biomass burning may be most important. The burned biomass is enriched in <sup>14</sup>C compared to the background. In particular, the wood growing in the time of the <sup>14</sup>C bomb-peak (ca. 50 years old) may add considerable <sup>14</sup>C load to the local carbon cycle. In the investigated area the biomass has been used for heating the houses and cooking by householders, and also used in industrial sector. Burning of <sup>14</sup>C-enriched biomass may suppress the Suess effect, thus the results showed a similar Δ<sup>14</sup>C value as Jungfraujoch, however, we are lacking the detailed statistical data for the Silesia.

In this study, we assessed the characteristics of pine needles exposed to multi-source pollution in Silesia and determined their carbon isotopic composition, WUE, and trace element concentrations in pine needles to verify the homogeneity of data obtained at 10 sampling sites near the heat and power plant in Łaziska, roads, and houses.

## MATERIALS AND METHODS

The sampling sites were located near the heat and power plant Łaziska (HPP Łaziska) in a multi-source pollution industrial area (Figure 1; Table 1). Two of these sampling sites (S4 and S5) were the same as those investigated in 2012–2014 (Sensula et al. 2021). In this study, pines growing at 10 sampling sites located at different distances from factories, roads, and households were investigated. Nine of them were located (S1, S2, S3, S4, S5, S6, S10, S12, S14) at distances of 2 to ca. 20 km from HPP Łaziska. The sampling sites were selected to be near the streets and considering the direction of the dominant southwestern winds. Sites S10 and S5 are located close to the road no. 81 (on the west of the road), site S14 is located close to the route no. 81 (on the east of the road), site S1 is located close to the road no. 86 (on the west of the road) and site S3 is located close to the road S1 (on the north of the road). A comparative site (S7) was located in Gliwice nearby road no. 902. Sites S2 and S12 were located deep in the forests: Lasy Murckowskie and Lasy Pszczyńskie, respectively. Samples of one-year-old needles that began growing in 2020 were collected in April 2021, on the same day to avoid weather influences. Needles were collected from the tree crowns of 20-year-old Scots pine (*Pinus Sylvestris* L.), placed in plastic bags, and separated manually in the laboratory.

### Carbon Isotope Analysis

The dried needles were extracted using a Soxhlet column to remove waxes and resins with the following solvents: Toluene (100°C, 4 hr), ethanol (100°C, 4 hr), and water (100°C, 4 hr). Next, the samples were rinsed in hot water until they were neutralized and dry. α-Cellulose was extracted by applying procedures based on Green's method (1963) used in the mass spectrometry laboratory of the Silesian University of Technology (Pazdur et al. 2013; Sensula and Pazdur 2013). Old wood ("Olga") to be used as the background material was

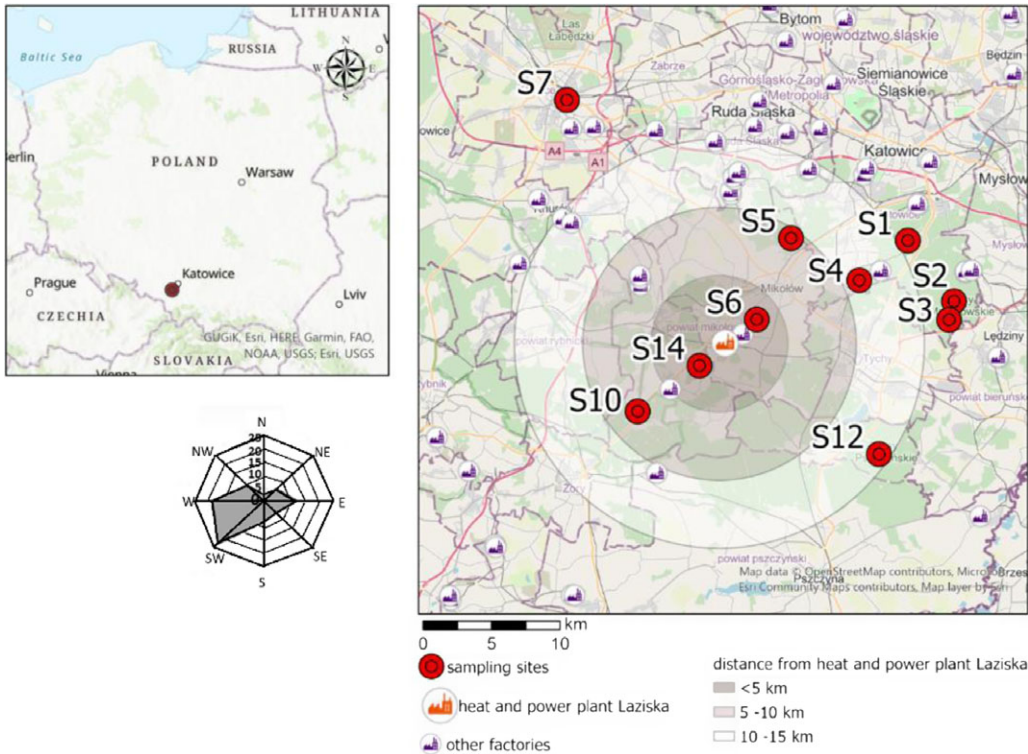


Figure 1 Sampling sites and localization of the factories in the investigated area (the location of other factories is based on data from gugik.gov.pl).

subjected to the same  $\alpha$ -cellulose extraction procedure.  $\delta^{13}\text{C}$  was determined at the mass spectrometry laboratory of the Silesian University of Technology using an Isoprime continuous-flow isotope ratio mass spectrometer (GV Instruments, Manchester, UK). The standard deviation of the repeated analysis of internal standards (C-3 and C-5, IAEA) was better than 0.2‰.

The relative deviation of the isotopic composition is expressed in parts per thousand (‰, VPDB) as:

$$\delta = (R_{\text{sample}}/R_{\text{standard}} - 1) \cdot 1000$$

The intrinsic WUE, which is directly linked to the ratio of intercellular ( $c_i$ )-to-atmospheric ( $c_a$ )  $\text{CO}_2$  ( $c_i/c_a$ ), was calculated according to the equations:

$$\Delta^{13}\text{C}_{\text{cel}} = \left( \frac{\delta^{13}\text{C}_{\text{air}} - \delta^{13}\text{C}_{\text{cel}}}{1 + \frac{\delta^{13}\text{C}_{\text{cel}}}{1000}} \right)$$

Table 1 Sampling site locations in the Silesia region.

| Site name | Commune/ forestry          | Longitude  | Latitude   | Distance to power plant (km) | Distance to nearest residential area (km) | Distance to nearest industrial site (km) | Distance to nearest road (km) |
|-----------|----------------------------|------------|------------|------------------------------|---|--|-------------------------------|
| S1        | Ochojec                    | 19°1'58"E  | 50°12'0"N  | 15                           | 0.6                                       | 2.7                                      | 0.7                           |
| S2        | Ledziny I (Murcki Forest)  | 19°4'48"E  | 50°9'36"N  | 17                           | 2.3                                       | 2.3                                      | 1.9                           |
| S3        | Ledziny II (Murcki Forest) | 19°4'30"E  | 50°8'53"N  | 16                           | 1.3                                       | 3.7                                      | 0.8                           |
| S4        | Podlesie                   | 18°58'58"E | 50°10'26"N | 11                           | 1.4                                       | 1.7                                      | 0.9                           |
| S5        | Zadole                     | 18°54'46"E | 50°12'7"N  | 9                            | 1.7                                       | 5.1                                      | 0.8                           |
| S6        | Wry                        | 18°52'40"E | 50°8'53"N  | 3                            | 1.2                                       | 1.5                                      | 0.7                           |
| S7        | Gliwice                    | 18°40'58"E | 50°17'31"N | 21                           | 0.1                                       | 2.1                                      | 0.2                           |
| S10       | Woszycze                   | 18°45'25"E | 50°5'13"N  | 8                            | 0.3                                       | 2.9                                      | 0.1                           |
| S12       | Kobiór (Pszczyna Forest)   | 19°0'11"E  | 50°3'36"N  | 14                           | 3   | 8.7                                      | 1.6                           |
| S14       | Zawiść                     | 18°49'12"E | 50°7'1"N   | 2.5                          | 2   | 2.7                                      | 0.1                           |

Thus,

$${}_iWUE = \frac{A}{g_s} = \frac{ca - ci}{1.6} = c_a \frac{b - \Delta^{13}C_{cel}}{1.6(b - a)}$$

where  $\delta^{13}C_{cel}$  is the carbon isotope composition of plant cellulose, and  $\delta^{13}C_{air}$  is the carbon isotope composition of the air;  $a$  is the isotope fractionation during  $CO_2$  diffusion through stomata (4.4‰);  $b$  is the isotope fractionation during fixation by RuBisCO (27‰). The  $iWUE$  (intrinsic water-use efficiency) was derived from the carbon isotope composition of the needles and carbon isotope composition of atmospheric  $CO_2$ , where 1.6 is the molar diffusivity ratio of  $CO_2$ -to- $H_2O$  (i.e.,  $g_{CO_2} = g_{H_2O}/1.6$ ).

According to NOAA (NOAA 2021) the mean  $CO_2$  concentration in the air based on the monthly average between May 2020 and April 2021, when the needles were growing, was 412 ppm. A  $\delta^{13}C$  level of  $-8.47$ ‰ was calculated based on Graven's model (Graven et al. 2017).

Graphite for AMS radiocarbon measurements was prepared using an AGE-3 system (Wacker et al. 2010). Subsamples of ca. 3 mg of extracted  $\alpha$ -cellulose were packed into tin boats and combusted in a Vario Micro Cube (Elementar<sup>TM</sup>) elemental analyzer. The  $CO_2$  in a 1 mg sample of carbon was reduced by reaction with  $H_2$  in the presence of a Fe catalyst at 580°C. Oxalic Acid II (NIST SRM4990C), which was used as a modern reference material and background material, was prepared in the same manner.  $^{14}C$  concentrations were determined at the Poznan Radiocarbon Laboratory, Poland (Goslar et al. 2004).

The carbon modern fraction,  $F^{14}\text{C}$  or  $\Delta^{14}\text{C}$  value (‰), was calculated according to the equation below (van der Plicht and Hogg 2006):

$$\Delta^{14}\text{C} = (F^{14}\text{C} \cdot e^{-\lambda(T_i-1950)} - 1) \cdot 1000$$

where:  $F^{14}\text{C}$  is normalized radiocarbon concentration;  $\lambda$  is decay constant for radiocarbon isotope equal to  $8267\text{yr}^{-1}$ ;  $T_i$  is calendar year.

The blank for “Olga”  $\alpha$ -cellulose was  $0.86 \pm 0.05$  pMC, which is higher than the usual coal blank value of 0.3 pMC obtained by the Gliwice AMS Laboratory. This was caused by elaborate multi-step chemical treatment of the material; however, for modern samples, the difference in the pMC value calculated using two blanks was negligible ( $< 0.01$  pMC).

### ICP-AES Analysis

The dried and ground (fraction size: 0.1 mm) needles were mineralized in a 65% solution of nitric acid ( $\text{HNO}_3$ ) and 37% solution of hydrochloric acid (HCl) in a 1:4 proportion using a UniClever microwave mineralizer (Ayrault, 2005). The process was repeated twice for each sample (for replication purposes). The prepared solutions were subjected to Cr, Co, Ni, Cu, Zn, Sr, Ba, and Pb analysis using a JY 2000 – Sequential ICP-AES spectrometer (Jobin Yvon). The repeatability of measurements was controlled by replicating the preparations and measurements for each sample twice. Additional analyses for sample S1-1 were duplicated to verify if the instrument was correctly calibrated. The results of duplication and variability were satisfactory for each element (RSD  $< 10\%$ ), meaning that the spectrometer provided reliable and repeatable data. The detection limits are shown in Table 2.

## RESULTS AND DISCUSSION

### $\delta^{13}\text{C}$

Variations in the isotopic composition of the pine needles may be due to fossil fuel combustion and the mixing of  $\text{CO}_2$  in the atmosphere. The higher  $\text{CO}_2$  concentration affects  $\delta^{13}\text{C}$  and thus iWUE. The result of the “blending” of carbon isotopes origin from different sources is depletion of  $\delta^{13}\text{C}$  in atmospheric  $\text{CO}_2$  and in the biosphere. According to Zimnoch et al. (2012), in southern Poland the  $\delta^{13}\text{C}$  in coal is  $\sim -24\%$ , and in petroleum products in gasoline is  $\sim -31\%$ . Although the observation made by Kawashima and Haneishi (2012) who  $\delta^{13}\text{C}$  linked to suspended particulate matter from biomass combustion ( $\text{C}_3$  plants) shown that could varied between  $-35$  to  $-28\%$ , there is little chance that the observed variability of  $\delta^{13}\text{C}$  in needle cellulose arises from aerosols deposited on the surface of the needles, but the  $\text{CO}_2$  origin from biomass compustion in this region cannot be excluded. In 2008, Górká et al. (2011), had noted that  $\delta^{13}\text{C}$  in gasoline car was  $-31.7\%$ , in diesel car was  $-31.9\%$ , in liquid petroleum gas car was  $-33.5\%$ , in coal burning chimney was  $-24.1\%$ , in wood burning chimney was  $-28.1\%$  and in natural gas burning chimney was  $-29.8\%$ , respectively. In 2021, we have observed that the  $\delta^{13}\text{C}$  in pine needles fluctuate between  $-30.2$  to  $-27.3\%$ . The spatial distribution of  $\delta^{13}\text{C}$  in pine needles can be associate with emission of carbon dioxide connected with different human activities (Figure 2b).

Less negative  $\delta^{13}\text{C}$  ( $\sim -27\%$ ) values have been observed in pine growing close to the edge of the forests and near to the residential area (S7, S10, S1, S6). We cannot exclude that in the

Table 2 Detection limits for ICP-AES, JY 2000.

| Element | Detection limit ( $\mu\text{g}/\text{kg}$ ) |
|---------|---|
| Cr      | 0.7   |
| Co      | 0.5   |
| Ni      | 0.3   |
| Cu      | 0.35  |
| Zn      | 0.3   |
| Sr      | 0.5   |
| Ba      | 0.4   |
| Pb      | 1.1   |

residential area not only coal but also biomass may be used by citizens during cooking and heating houses. A distance between these sampling sites and the nearest residential area is less than 1.5 km. The most negative  $\delta^{13}\text{C}$  ( $\sim -30\%$ ) values was observed in S14, S3, and S5 located close to the edge of the forests and near the road (less than 1 km) and farther from residential area (1.5–2.5 km). In site S4, it has been observed that carbon dioxide can origin from different sources. This site is at the same distance from the nearest road and residential area as S3, however this site is nearer to the nearest industrial factory. Despite the fact that the site S7 has been very close to the street, the effect of gasoline combustion by cars has not been observed in  $\delta^{13}\text{C}$  in trees growing there. It can be associated with a fact that the pines, at S7, grow behind a sound screen, which can be an important barrier not only for the noise but also for distribution of contamination emitted by traffic. In the investigated area we cannot observe a direct link between variation in  $\delta^{13}\text{C}$  in pines and distance from power plant to sampling stands (Figures 3a and 3b). That can be due to a fact that most of the industrial factories have been implemented pro-ecological policy since the 1990s. Detailed spatial analysis showed that the variation in  $\delta^{13}\text{C}$  in pines may be linked with other human activities such as residential heating and cooking, including not only coal but also biomass combustion or road traffic and petroleum and gas combustion.

$\delta^{13}\text{C}$  in pine growing in the sampling sites located deep in the forest (S2,S12) was equal to  $-29\%$ . This value may be probably a result of the “blending” of carbon isotopes origin from different sources. In this moment it cannot be excluded, another hypothesis, that these sampling sites are too far from potential local emitters, to record local signal connected householders and traffic, and these  $\delta^{13}\text{C}$  values could be associated with long-range transport of air contamination and depletion of  $\delta^{13}\text{C}$  in the atmosphere.  $\delta^{13}\text{C}$  values in the needles of pines depend on time and localization of the sampling sites. The stomata co-regulate the influx of  $\text{CO}_2$  for photosynthesis and the transpirational loss of water to the atmosphere. According to Asseng (Asseng et al. 2015), the increasing  $\text{CO}_2$  may positively impact the  $\delta^{13}\text{C}$  and  $i\text{WUE}$  of  $\text{C}_3$  species. (In the tree rings, an increase in  $i\text{WUE}$  has been noted at the local and global scales since the 1960s, which implies an associated modification to the local carbon and/or hydrological cycles [Loader et al. 2011]). In Silesia, the level of  $i\text{WUE}$  in pine needles was between 44 and 73  $\mu\text{mol}/\text{mol}$  in 2012 (the needles created in 2012 and collected in January 2013), between 45–66  $\mu\text{mol}/\text{mol}$  in 2013 (the needles created in 2013 and collected in September 2013), and 46–81  $\mu\text{mol}/\text{mol}$  in 2014 (the needles created in 2014 and collected July 2014) (Sensula 2015). In Silesia in 2021, we have noted that  $i\text{WUE}$  is not constant and  $i\text{WUE}$  ranged from ca. 60 (S3, S5, S14) to ca. 90  $\mu\text{mol}/\text{mol}$ . The lowest  $i\text{WUE}$  value was observed in sites (S3, S5 and S14) located in close

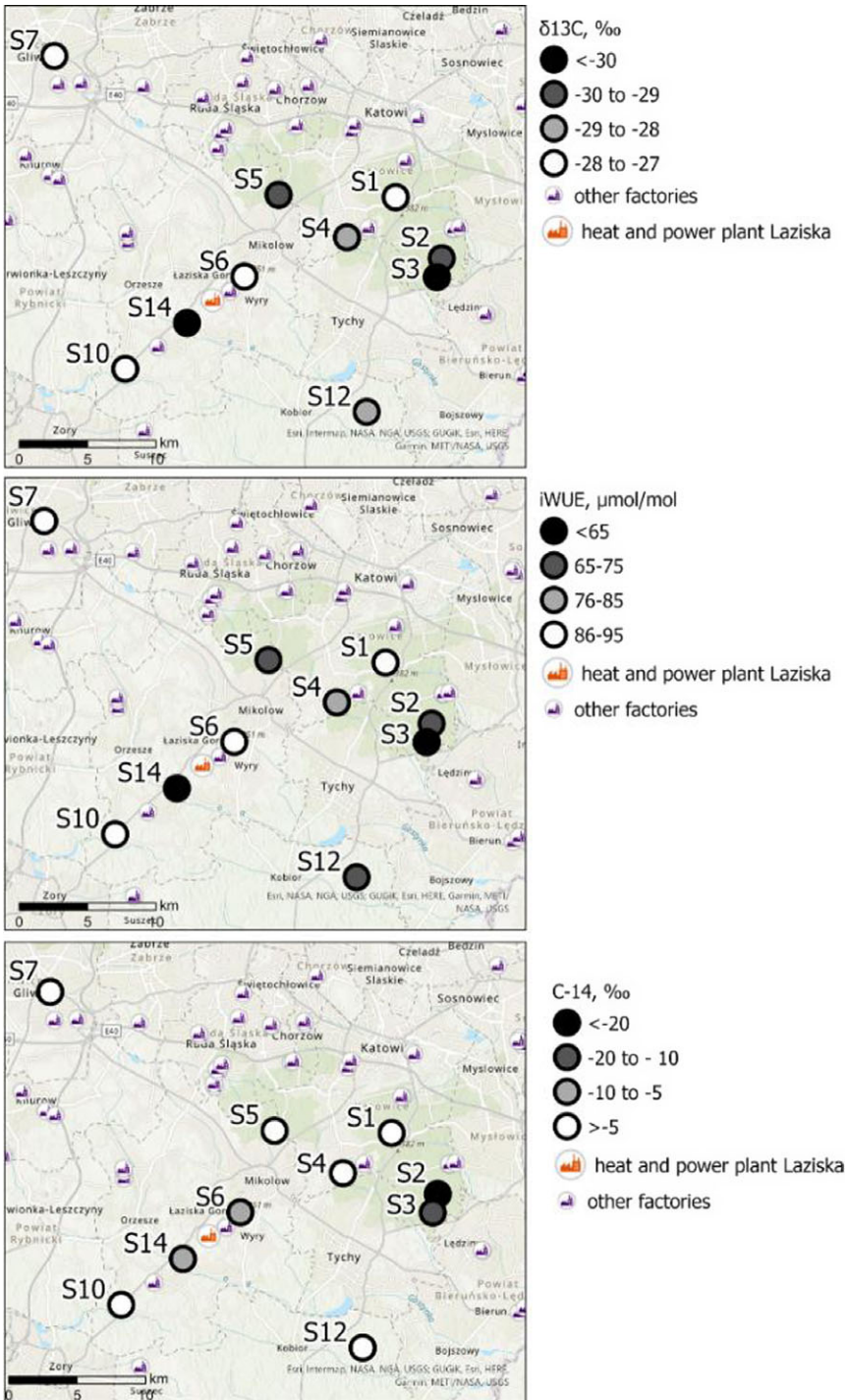


Figure 2a Top image: Spatial variation in the stable carbon isotopic composition of the one-year-old pine needles collected in Silesia in 2021; middle image: spatial variation in iWUE of the one-year-old pine needles collected in Silesia in 2021; bottom image: spatial variation in the  $^{14}\text{C}$  of the one-year-old pine needles collected in Silesia in 2021.

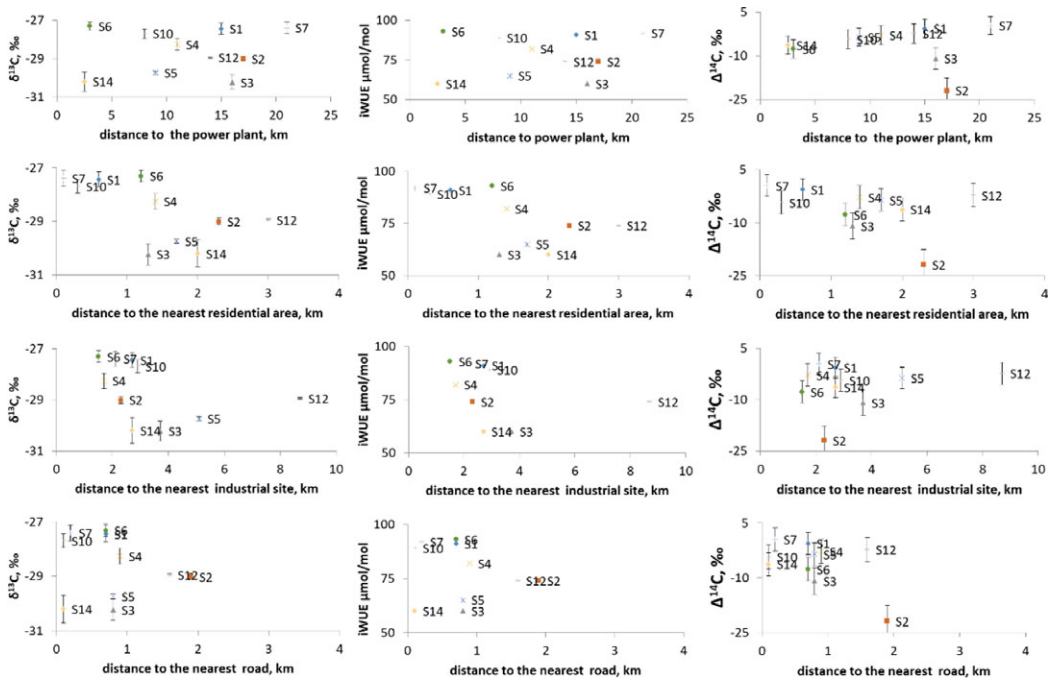


Figure 2b Spatial variation in the carbon isotopic composition and iWUE of the one-year-old pine needles collected in Silesia in 2021.

approximately to the streets and the highest iWUE value in the sites localized near the residential area (S1, S6, S7, S10).

### Radiocarbon

The samples had a consistent average carbon content of 44%. The  $\Delta^{14}\text{C}$  values were calculated for 2020. A high variation of  $\Delta^{14}\text{C}$  was observed from  $-21.9\text{‰}$  to  $+0.5\text{‰}$  (Table 3). The  $^{14}\text{C}$  concentration in “clean air” was estimated to be  $\Delta^{14}\text{C}_{\text{JFJ}} = -1.5 \pm 0.48\text{‰}$ , based on data from Jungfraujoch (Emmenegger et al. 2021) extrapolated to 2020. Most of the investigated sites (except for sites S1 and S7) have lower  $\Delta^{14}\text{C}$  than  $\Delta^{14}\text{C}_{\text{JFJ}}$ , indicating a local Suess effect. The fraction of fossil carbon (FFCO<sub>2</sub>) calculated according to Piotrowska et al. (2020) increased from  $-0.2$  to  $+2\%$  and was  $+0.45 \pm 0.62\%$  on average. These values are consistent with FFCO<sub>2</sub> obtained for pine needles growing near the Laziska power plant in AD 2013:  $-0.21 \pm 0.05\%$  for S4 and  $-0.82 \pm 0.08\%$  for S5 (Sensula et al. 2018). Also, the FFCO<sub>2</sub> determined for the tree rings around Gliwice City for AD 2008–2012 ranged from  $-0.23$  to  $+0.89\%$  (Piotrowska et al. 2020). At some sampling sites,  $\Delta^{14}\text{C}$  seems to be higher than the  $\Delta^{14}\text{C}$  concentration in clean air in the Alps. A similar effect was observed in this region in 2012–2014 (Sensula et al. 2021) and for some sites near Gliwice city (Piotrowska et al. 2020).

### Elemental Analysis

The average concentrations of heavy metals in collected samples are presented in Table 4. These concentrations followed the order  $\text{Zn} > \text{Cu} > \text{Pb} > \text{Cr}$ , which was consistent with a

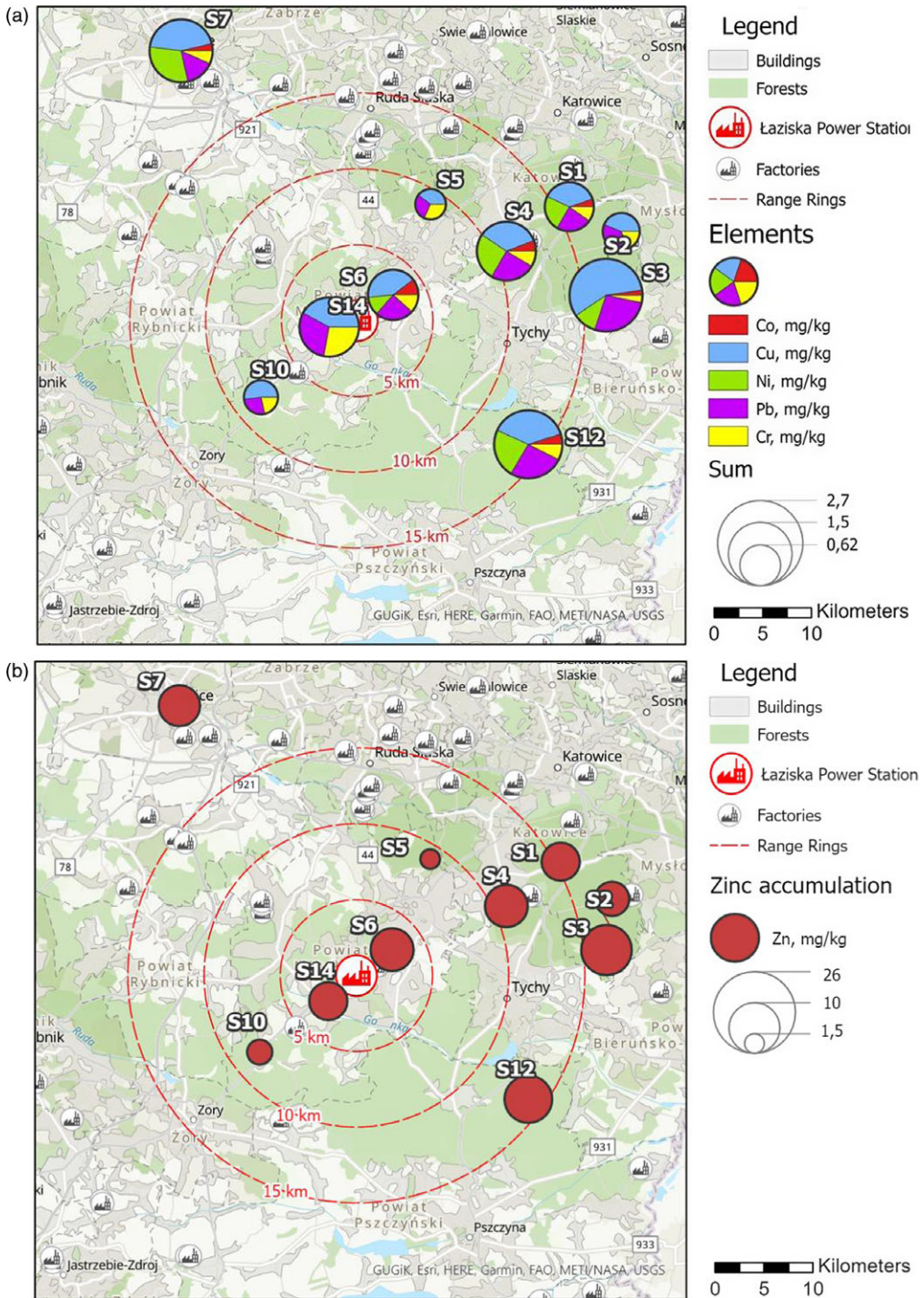


Figure 3 (a) Accumulation of Cr, Co, Ni, Pb, and Cu in *Pinus Sylvestris* L. needles located different distances from pollution emitters (Łaziska Power Plant, other industrial sites, and residential areas). (b) Accumulation of Zn in *Pinus Sylvestris* L. needles located different distances from pollution emitters (Łaziska Power Plant, other industrial sites, and residential areas).

Table 3 The carbon isotope results of 1-year-old pine needles grown in 10 sampling sites (S1, S2, S3, S4, AS5, S6, S7, S10, S12, S14) in a multi-point air pollution source area in Silesia in 2021. The data of the previous analysis (Sensula et al. 2018, 2021) of 1-year-old pine needles formed in 2012 collected in 2013 (winter) and growing in S4 and S5 are marked by \*, year-to-year differences in carbon isotopic composition of the needles is marked as  $\Delta$ .

| Site                          | Lab code    | $\Delta^{14}\text{C}$ ‰ | FFCO <sub>2</sub> ‰ | $\delta^{13}\text{C}$ ‰ | iWUE $\mu\text{mol/mol}$ |
|-------------------------------|-------------|-------------------------|---------------------|-------------------------|--------------------------|
| S1                            | PBL_2021_2  | $-0.6 \pm 3.1$          | $-0.09 \pm 0.03$    | $-27.44 \pm 0.29$       | 91                       |
| S2                            | PBL_2021_4  | $-21.9 \pm 4.3$         | $2.04 \pm 0.04$     | $-29.01 \pm 0.13$       | 74                       |
| S3                            | PBL_2021_6  | $-10.9 \pm 3.1$         | $0.94 \pm 0.04$     | $-30.23 \pm 0.39$       | 60                       |
| S4                            | PBL_2021_8  | $-2.8 \pm 3.3$          | $0.13 \pm 0.03$     | $-28.26 \pm 0.30$       | 82                       |
| S5                            | PBL_2021_10 | $-3.6 \pm 3.1$          | $0.21 \pm 0.03$     | $-29.74 \pm 0.09$       | 65                       |
| S6                            | PBL_2021_12 | $-7.7 \pm 3.2$          | $0.62 \pm 0.03$     | $-27.31 \pm 0.22$       | 93                       |
| S7                            | PBL_2021_14 | $0.5 \pm 3.3$           | $-0.20 \pm 0.03$    | $-27.39 \pm 0.17$       | 92                       |
| S10                           | PBL_2021_20 | $-4.3 \pm 3.3$          | $0.28 \pm 0.03$     | $-27.69 \pm 0.25$       | 89                       |
| S12                           | PBL_2021_24 | $-2.3 \pm 3.3$          | $0.08 \pm 0.03$     | $-28.946 \pm 0.03$      | 74                       |
| S14                           | PBL_2021_28 | $-6.3 \pm 3.2$          | $0.49 \pm 0.03$     | $-30.20 \pm 0.50$       | 60                       |
| S4*                           | LA_9        | $33.1 \pm 5.1$          | $-0.21 \pm 0.05$    | $-28.6 \pm 0.09$        | 73                       |
| S5*                           | LA_10       | $39.4 \pm 8.1$          | $-0.82 \pm 0.08$    | $-31.2 \pm 0.01$        | 45                       |
| $\Delta\text{S4}_{2021-2013}$ |             | $35.9 \pm 6.1$          | $0.33 \pm 0.13$     | 0.34                    | 9                        |
| $\Delta\text{S5}_{2021-2013}$ |             | $43.0 \pm 8.7$          | $1.03 \pm 0.21$     | 1.46                    | 20                       |

previous study performed for the Silesian industrial region (Sensula et al. 2021). In this study, high concentrations of Cu, Ni, and Pb were obtained in all samples, indicating that the Silesian region is characterized by unfavorable air conditions in terms of plant health. Especially high concentrations of Zn, Cu, and Pb were obtained at sites S3, S4, and S12 (up to 237% concentration relative to the mean obtained in the whole study for a given element) (Table 4). The concentrations of the elements measured in pin needles were lower than results of the research by Pietrzykowski et al. in 2009 (Pietrzykowski et al. 2014), in which the average heavy metal concentrations in pine needles were as follows: Zn from 33 to 77 mg/kg, Cu from 3.0 to 28 mg/kg, and Pb from 0.8 to 3.2 mg/kg. The results of studies conducted by other authors vary greatly, and the metal content depends on the species of needle and the region, for example in Poland (Gamrat and Ligocka 2018) in three research areas: Świeradów Zdrój, Świnoujście, Byszyno, Zn range from 46.29 mg/kg to 151.72 mg/kg, Pb range from 0.05 mg/kg to 2.96 mg/kg, Cr from 2.38 mg/kg to 6.18 mg/kg, Ni from 4.22 mg/kg to 36.53 mg/kg, Co from 0.04 mg/kg to 0.65 mg/kg. In another study, the concentrations of heavy metals in the needles of different pine species varied, with Cu ranging from 7 to 10 mg/kg, Ni from 41 to 90 mg/kg, and Zn from 42 to 119 mg/kg (Parzych et al. 2017).

According to a study performed in coal mining regions (Pietrzykowski et al. 2014), high concentrations of these heavy metals were recorded near coal mines. After investigating sites S3 and S4, it was established that both sites were relatively close to two coal mines, KWK Wesola and KWK Staszic-Murcki (site S3 was located < 5 km from KWK Wesola, and site S4 < 7 km from KWK Staszic-Murcki). These results indicates that dust rich in heavy metals released from the mines could be absorbed by plants growing at the collection

Table 4 The results of trace element concentrations in 1-year-old pine needles grown in 10 sampling sites in a multi-point air pollution source area in Silesia. Values below the detection limit are marked as \*. The data of the previous analysis of 1-year-old pine needles formed in 2012 collected in 2013 (winter) and growing in S4 and S5 are marked as \*.

| Site | Lab code    | <Cr><br>mg/kg | u(<Cr>)<br>mg/kg | <Co><br>mg/kg | u(<Co>)<br>mg/kg | <Ni><br>mg/kg | u(<Ni>)<br>mg/kg | <Cu><br>mg/kg | u(<Cu>)<br>mg/kg | <Zn><br>mg/kg | u(<Zn>)<br>mg/kg | <Sr><br>mg/kg | u(<Sr>)<br>mg/kg | <Ba><br>mg/kg | u(<Ba>)<br>mg/kg | <Pb><br>mg/kg | u(<Pb>)<br>mg/kg |
|------|-------------|---------------|------------------|---------------|------------------|---------------|------------------|---------------|------------------|---------------|------------------|---------------|------------------|---------------|------------------|---------------|------------------|
| S1   | PBL_2021_2  | 0.0875        | 0.0020           | 0.0455        | 0.0028           | 0.2110        | 0.0080           | 0.339         | 0.016            | 5.655         | 0.014            | 6.17          | 0.24             | 6.61          | 0.22             | 0.2100        | 0.0020           |
| S2   | PBL_2021_4  | 0.09          | 0.50             | —             | —                | —             | —                | 0.224         | 0.018            | 4.61          | 0.18             | 2.57          | 0.19             | 3.120         | 0.092            | 0.1910        | 0.0038           |
| S3   | PBL_2021_6  | 0.0655        | 0.0014           | 0.0445        | 0.0014           | 0.207         | 0.010            | 1.13          | 0.23             | 9.85          | 0.24             | 4.13          | 0.16             | 4.535         | 0.012            | 0.528         | 0.031            |
| S4   | PBL_2021_8  | 0.1105        | 0.0028           | 0.0760        | 0.0020           | 0.338         | 0.012            | 0.45          | 0.25             | 7.05          | 0.17             | 4.12          | 0.21             | 4.39          | 0.23             | 0.3200        | 0.0037           |
| S5   | PBL_2021_10 | 0.1115        | 0.0023           | —             | —                | —             | —                | 0.140         | 0.010            | 1.50          | 0.12             | 0.226         | 0.012            | 0.554         | 0.005            | 0.0985        | 0.0012           |
| S6   | PBL_2021_12 | 0.111         | 0.016            | 0.0980        | 0.0034           | 0.1135        | 0.0066           | 0.391         | 0.012            | 7.15          | 0.18             | 2.10          | 0.22             | 2.34          | 0.15             | 0.234         | 0.020            |
| S7   | PBL_2021_14 | 0.0985        | 0.0012           | 0.0545        | 0.0012           | 0.450         | 0.014            | 0.656         | 0.011            | 6.57          | 0.15             | 0.983         | 0.028            | 1.250         | 0.056            | 0.2210        | 0.0061           |
| S10  | PBL_2021_20 | 0.093         | 0.010            | —             | —                | —             | —                | 0.225         | 0.017            | 2.46          | 0.19             | 0.565         | 0.032            | 0.990         | 0.022            | 0.117         | 0.010            |
| S12  | PBL_2021_24 | 0.1290        | 0.0093           | 0.0855        | 0.0046           | 0.403         | 0.011            | 0.662         | 0.024            | 8.775         | 0.069            | 1.20          | 0.23             | 1.67          | 0.26             | 0.450         | 0.012            |
| S14  | PBL_2021_28 | 0.37          | 0.55             | —             | —                | —             | —                | 0.553         | 0.015            | 5.64          | 0.24             | 0.749         | 0.046            | 1.100         | 0.020            | 0.394         | 0.013            |
| S4*  | LA5_5_2012  | 0.082         | —                | 0.048         | —                | —             | —                | 0.87          | —                | 11.1          | —                | 1.78          | —                | 0.7           | —                | 0.138         | —                |
| S5*  | LA_10_2012  | 0.136         | —                | 0.075         | —                | 0.26          | —                | 1.02          | —                | 7.0           | —                | 1.72          | —                | 1.76          | —                | 0.132         | —                |

sites. Site 12 was located farther (~14 km) from KWK Wesola, but another coal mine, KWK Piast (distance ~10 km) was located near site S12. Thus, the higher concentrations of heavy metals in sample from site 12 than in other collected samples (Table 4) were possibly related to mining facilities in the region.

## CONCLUSIONS

Trees can be used in biomonitoring of the environment. The determination of foliage properties may be important for analyzing local and regional changes in environments affected by contaminants originating from different sources. Variations in carbon isotope in pine needles may occur due to a mixture of air contaminants originating mostly from different sources (coal, gasoline, burning of biomass), which has been used for heating the houses and cooking by householders and also in different industrial sectors. This is probably the reason why radiocarbon concentration in the needles samples shows a similar value as Jungfrauoch.

The  $^{14}\text{C}$  do not show any variation, except in some specific sites, whereas the spatial variability in  $\delta^{13}\text{C}$  (3‰) is greater than the temporal one (0.3–1.5‰), suggesting variability in carbon stable isotopes could be mostly related to local effects. The analysis of the stable isotopes composition in the needles showed the fluctuation in carbon isotopic composition due to gasoline (linked to traffic) and coal combustion (linked to householders and industry). The  $\delta^{13}\text{C}$  in pines growing close to the edge of the forest and close to the roads has been less negative ( $\delta^{13}\text{C}$  is equal to ca.  $-27\%$ ) whereas  $\delta^{13}\text{C}$  in pines growing close to the edge of the forest and close to the heating and cooking at residential area has been more negative ( $\delta^{13}\text{C}$  is equal to ca.  $-30\%$ ) when compared to the  $\delta^{13}\text{C}$  in pines growing deep in the forest, where  $\delta^{13}\text{C}$  was equal to  $-29\%$ . Further additional analyses would help to improve our understanding of the variability of  $^{13}\text{C}$  and  $^{14}\text{C}$  in pine foliages.

The elements of the concentrations in pine needles varied widely, and the temporal and spatial variations were evident. The obtained results indicate that the heavy metals' concentration in the samples of needles was relatively high and it decreased with the distance from the pollution emitters.

## ACKNOWLEDGMENTS

This study was a part of the Project-Based Learning “Applied Physics and ArcGIS technology in the Environmental Research-Air pollutants accumulation the foliage – a case study of biomonitoring of the industrial area (ACCUM)” (PI: Barbara Sensula, Team Leader: Dawid Lazaj). The research was supported by the Ministry of Science and Education through a special grant for the  $^{14}\text{C}$  and Mass Spectrometry Laboratory (209848/E-367/SPUB/2018/1).

## REFERENCES

- Asseng S, Ewert F, Martre P, Rötter RP, Lobell DB, Cammarano D, Kimball BA, Ottman MJ, Wall GW, White JW, et al. 2015. Rising temperatures reduce global wheat production. *Nature Climate Change* 5:143–147. doi: [10.1038/nclimate2470](https://doi.org/10.1038/nclimate2470).
- Ayrault S. 2005. Multi-element analysis of plant and soil samples. Trace and ultratrace elements in plants and soils, hyper article en Ligne - Sciences de l'Homme et de la Société. <https://hal.archives-ouvertes.fr/hal-02651214>.

- Barszczowska L, Jędrysek MO. 2005. Carbon isotope distribution along pine needles (*Pinus Nigra Arnold*). Acta Societatis Botanicorum Poloniae 74:93–98.
- Brendel O, Handley K, Griffiths H. 2003. The  $\delta^{13}\text{C}$  of Scots pine (*Pinus sylvestris* L.) needles: spatial and temporal variations. Annals of Forest Science, Springer Nature (since 2011)/EDP Science (until 2010) 60(2):97–104. [ff10.1051/forest:2003001ff.fhal-00883681f](https://doi.org/10.1051/forest:2003001ff.fhal-00883681f).
- Cherubini P, Battipaglia G, Innes JL. 2021. Tree vitality and forest health: can tree-ring stable isotopes be used as indicators? Current Forestry Reports 7:69–80.
- Emmenegger L, Leuenberger M, Steinbacher M, ICOS RI. 2021. ICOS ATC/CAL  $^{14}\text{C}$  release, Jungfrauoch (10.0 m), 2016-01-04–2019-08-12. Available at: <https://hdl.handle.net/11676/JjmhH4pUyWlbqTAAx4x54deg>.
- Gamrat R, Ligocka K. 2018. Stężenia wybranych metali ciężkich w igłach sosny zwyczajnej z wybranych obszarów Polski. Inżynieria Ekologiczna 19(1):61–65. doi: [10.12912/23920629/81653](https://doi.org/10.12912/23920629/81653).
- Gilbert ME, Zwieniecki MA, Holbrook NM. 2011. Independent variation in photosynthetic capacity and stomatal conductance leads to differences in intrinsic water use efficiency in 11 soybean genotypes before and during mild drought. Journal of Experimental Botany 62(8):2875–2887. doi: [10.1093/jxb/erq461](https://doi.org/10.1093/jxb/erq461).
- Górka M, Sauer PE, Lewicka-Szczebak D, Jędrysek M-O. 2011. Carbon isotope signature of dissolved inorganic carbon (DIC) in precipitation and atmospheric  $\text{CO}_2$ . Environmental Pollution 159(1):294–301. doi: [10.1016/j.envpol.2010.08.027](https://doi.org/10.1016/j.envpol.2010.08.027).
- Goslar T, Czernik J, Goslar E. 2004. Low-energy  $^{14}\text{C}$  AMS in Poznan Radiocarbon Laboratory, Poland. Nuclear Instruments and Methods in Physics Research B 223–224:5–11.
- Graven H, Allison CE, Etheridge DM, Hammer S, Keeling RF, Levin I, Meijer HAJ, Rubino M, Tans PP, Trudinger CM, Vaughn BH, White JWC. 2017. Compiled records of carbon isotopes in atmospheric  $\text{CO}_2$  for historical simulations in CMIP6. Geosci. Model Dev., 10:4405–4417. doi: [10.5194/gmd-10-4405-2017](https://doi.org/10.5194/gmd-10-4405-2017).
- Guerrieri R, Belmecheri S, Ollinger SV, Asbjornsen H, Jennings K, Xiao J, Stocker B, Martin M, Hollinger DY, Bracho-Garrillo R, Clark K, Dore S, Kolb T, Munger J, Novick K, Richardson AD. 2019. Disentangling the role of photosynthesis and stomatal conductance on rising forest water-use efficiency. Proc Natl Acad Sci USA 116 (34): 16909–16914.
- Hammer S, Levin I. 2017. Monthly mean atmospheric  $^{14}\text{C}$  at Jungfrauochand Schauinsland from 1986 to 2016 [data set, www document]. University Library Heidelberg. <https://doi.org/10.11588/data/10100>.
- Kawashima H, Haneishi Y. 2012. Effects of combustion emissions from the Eurasian continent in winter on seasonal  $\delta^{13}\text{C}$  of elemental carbon in aerosols in Japan. Atmospheric Environment 46: 568–579. doi: [10.1016/j.atmosenv.2011.05.015](https://doi.org/10.1016/j.atmosenv.2011.05.015).
- Keeling CD. 1973. Industrial production of carbon dioxide from fossil fuel and limestone: Tellus 25:174–198.
- Letts MG, Nakonechny KN, Van Gaalen KE, Smith CM. 2009. Physiological acclimation of *Pinus flexilis* to drought stress on contrasting slope aspects in Waterton Lakes National Park, Alberta, Canada. Canadian Journal of Forest Research 39(3):629–641.
- Loader NJ, Walsh RPD, Robertson I, Bidin K, Ong RC, Reynolds G, McCarroll D, Gagen M, Young GHF. 2011. Recent trends in the intrinsic water-use efficiency of ringless rainforest trees in Borneo. Philosophical Transactions: Biological Sciences 366(1582): 3330–3339. doi: [jstor.org/stable/23076297](https://doi.org/10.1098/rstb.2010.0297).
- Mook W, van der Plicht J. 1999. Reporting  $^{14}\text{C}$  activities and concentrations. Radiocarbon 41(3):227–239.
- NOAA. 2021. [https://gml.noaa.gov/webdata/ccgg/trends/co2\\_mm\\_mlo.txt](https://gml.noaa.gov/webdata/ccgg/trends/co2_mm_mlo.txt). Last accessed: July 6, 2021.
- Pandey B, Agrawal M, Singh S. 2014. Assessment of air pollution around coal mining area: Emphasizing on spatial distributions, seasonal variations and heavy metals, using cluster and principal component analysis. Atmospheric Pollution Research 5(1): 79–86.
- Parzych A, Mochnacki S, Sobisz Z, Kurhaluk N, Polláková N. 2017. Accumulation of heavy metals in needles and bark of *Pinus* species. Folia Forestalia Polonica 59:34–44.
- Pazdur A, Kuc T, Pawelczyk S, Piotrowska N, Sensuła BM, Różański K. 2013. Carbon isotope composition of atmospheric carbon dioxide in southern Poland: imprint of anthropogenic  $\text{CO}_2$  emissions in regional biosphere. Radiocarbon 55(2–3):848–864.
- Pietrzykowski M, Socha J, van Doorn N. 2014. Linking heavy metal bioavailability (Cd, Cu, Zn and Pb) in Scots pine needles to soil properties in reclaimed mine areas. Science of the Total Environment 470–477:501–510.
- Piotrowska N, Pazdur A, Pawelczyk S, Rakowski AZ, Sensuła B, Tudyka K. 2020. Human activity recorded in carbon isotopic composition of atmospheric  $\text{CO}_2$  in Gliwice urban area and surroundings (southern Poland) in the years 2011–2013. Radiocarbon 62(1): 141–156. doi: [10.1017/rdc.2019.92](https://doi.org/10.1017/rdc.2019.92).
- Rakowski A. 2011. Radiocarbon method in monitoring of fossil fuel emission. Geochronometria 38(4): 314–332.
- Sensuła B, Fagel N, Michczyński A. 2021. Radiocarbon, trace elements and Pb isotope composition of pine needles from a highly industrialized region in southern Poland. Radiocarbon 63(2):713–726. doi: [10.1017/RDC.2020.132](https://doi.org/10.1017/RDC.2020.132).

- Sensula B, Michczyński A, Piotrowska N, Wilczyński S. 2018. Anthropogenic CO<sub>2</sub> emission records in Scots pine growing in the most industrialized region of Poland from 1975 to 2014. *Radiocarbon* 60(4): 1041–1053. doi: [10.1017/RDC.2018.59](https://doi.org/10.1017/RDC.2018.59).
- Sensula B, Pazdur A. 2013. Influence of climate change on carbon and oxygen isotope fractionation factors between glucose and  $\alpha$ -cellulose of pine wood. *Geochronometria* 40(2):145–152.
- Sensula B, Wilczynski S, Opala M. 2015. Tree growth and climate relationship: dynamics of Scots pine (*Pinus Sylvestris* L.) growing in the near-source region of the combined heat and power plant during the development of the pro-ecological strategy in Poland. *Water Air and Soil Pollution* 226(7), article 220.
- Sensula BM. 2015. Spatial and short-temporal variability of  $\delta^{13}\text{C}$  and  $\delta^{15}\text{N}$  and water-use efficiency in pine needles of the three forests along the most industrialized part of Poland. *Water Air Soil Pollut.* 226(11):362. doi: [10.1007/s11270-015-2623-z](https://doi.org/10.1007/s11270-015-2623-z).
- Suess HE. 1955. Radiocarbon concentration in modern wood. *Science* 122(3166): 415–417.
- van der Plicht J, Hogg A. 2006. A note on reporting radiocarbon. *Quat. Geochronol.* 1(4):237–40.
- Wacker L, Nemeč M, Bourquin J. 2010. A revolutionary graphitisation system: Fully automated, compact and simple. *Nuclear Instruments and Methods in Physics Research B* 268(7–8):931–934.
- Zimnoch M, Jelen D, Galkowski M, Kuc T, Necki J, Chmura L, Gorczyca Z, Jasek A, Róžański K. 2012. Partitioning of atmospheric carbon dioxide over central Europe: composition. *Isotopes in Environmental and Health Studies* 48(3):421–433.